Post-Print

This is the accepted version of:

P. Ghignoni, D. Invernizzi, M. Lovera
Fixed-Dynamics Antiwindup Design: Application to Pitch-Limited Position Control of Multirotor Unmanned Aerial Vehicles
IEEE Transactions on Control Systems Technology, In press - Published online 21/12/2020
doi:10.1109/TCST.2020.3042073

The final publication is available at https://doi.org/10.1109/TCST.2020.3042073

Fixed-dynamics anti-windup design: application to pitch-limited position control of multirotor Unmanned Aerial Vehicles

Pietro Ghignoni, Davide Invernizzi, Marco Lovera

***Abstract*—In this paper we present and validate an anti-windup control design suitable to deal with saturated discrete-time linear plants. Following the modern approach to anti-windup design, the proposed synthesis procedure is based on the compensator paradigm in which the anti-windup controller acts on top of a baseline one, tuned to achieve desirable performance in the unsaturated regime. After extending existing ideas for continuous-time plants to their discrete-time counterparts, the design of the anti-windup compensator is carried out with a focus on computational efficiency and optimized performance in practical operating scenarios. The proposed approach allows one to design fixed-dynamics anti-windup compensators for possibly open-loop unstable plants using generalized sector conditions. Then, the synthesis procedure is applied to tune a fixed-dynamics compensator having the structure of a static compensator cascaded with a unit delay to avoid algebraic loops. Finally, the benefits of such anti-windup augmentation are assessed experimentally to counteract windup effects arising in the position control of multirotor UAVs when pitch limitations are imposed.**

***Index Terms*—UAVs, multirotor, LMI, sector condition, anti-windup synthesis, position control**

I. Introduction

The design of high performance controllers for systems with input saturation is a challenging problem, even when linear plants are considered. This subject and the related "windup" problem, namely, the possible loss of stability and performance in some control systems due to actuation limitations, is motivated by the ubiquitous presence of saturation in practical applications. Modern anti-windup (AW) techniques [1]–[3] have been developed consistently in the last two decades to tackle the windup problem in a systematic way, *i.e.*, with formal stability and performance guarantees. For linear systems affected by actuator saturation, the modern approach to AW design is based on the introduction of a compensator acting on top of a baseline controller only when saturation occurs, aiming to prevent an excessive degradation of performance during saturation and to quickly recover the nominal behavior after saturation occurred.

Several approaches are now available to systematically tune AW compensators under stability and $\mathscr{L}_2$ performance optimization criteria [2]–[4]. These methods are typically based on the solution of Linear Matrix Inequalities (LMIs) aiming to enforce closed-loop stability while minimizing the $\mathscr{L}_2$ gain between the input and a suitable performance variable. However, as noted in [5], these techniques are not tailored to effectively address windup problems arising in many practical applications and could be overly conservative when tested on specific reference signals: the class of $\mathscr{L}_2$-bounded signals is quite large while most of the times actual reference signals are step-like functions.

In view of this, we first extend the performance-oriented fixed-dynamics AW synthesis procedure developed for continuous-time systems in [5] to its discrete-time counterpart, which is the natural setting for digital controller implementation. Using generalized sector conditions [6], we cast the AW design as a LMI-based optimization problem in which the performance index to be minimized penalizes the mismatch between the actual and the baseline closed-loop response with the reference signal generated by a stable filter that approximates a signal of interest [5]. The proposed approach can be used to tune, *e.g.*, AW controllers having the structure of a static compensator cascaded with a unit delay, which allows avoiding by design algebraic loops. In this way, one can easily implement such a computationally efficient compensator without impacting negatively on the designed performance, as a purely static AW compensator would do in practice when implemented with the delay [7]. In the second part of the paper, the proposed compensator design is used to augment the baseline controller of a quadrotor Unmanned Aerial Vehicle (UAV) in which saturation is fictitiously introduced to prevent excessive pitching of the platform. This limitation is often included in flight control systems of multirotors (*e.g.*, [8]) to avoid achieving too high speed. As shown in dedicated experiments, the baseline controller of the considered quadrotor is significantly affected by windup phenomena due to the presence of saturation, in particular, the set-point tracking performance is characterized by large overshoots. Instead, the AW compensator tuned according to the proposed synthesis procedure delivers excellent performance at the expense of a mild increase in the computational effort with respect to the baseline architecture. Besides the computational efficiency gained by using a low-order AW compensator [9], the main motivation for using the proposed performance-oriented AW design over suitable existing AW approaches is that we aim to address windup effects which appear when specific reference signals are commanded, notably step-like references, which is one the most common operating scenario for quadrotors. While other modern AW designs would be applicable as well in the considered application, *e.g.*, those proposed in [6],

P. Ghignoni, D. Invernizzi, M. Lovera are with Department of Aerospace Science and Technology, Politecnico di Milano, Via La Masa 34, 20156, Milano, Italy. Email to: pietro.ghignoni@mail.polimi.it, {davide.invernizzi, marco.lovera}@polimi.it

[10], [11], embedding a filter replicating reference signals of interest allows optimizing the performance in cases of practical interest, as supported also by the motivation and simulation results presented in [5].

The remainder of the paper is organized as follows. Section II presents the main notations used throughout the manuscript. Section III introduces the modern approach to AW compensator design for saturated linear plants in the discrete-time setting. In Section IV, the performance-oriented AW problem is first formulated and then the main theoretical results of the paper for the synthesis of fixed-dynamics AW compensators are reported and demonstrated. Section V shows the application of such results to a specific anti-windup compensator. In Section VI, after a brief description of the UAV used in the experiments, simulation and flight test results are reported and discussed. Section VII concludes the paper.

II. Notation

Notation. In this paper $\mathbb{Z}(\mathbb{Z}_{>0},\mathbb{Z}_{\geq 0})$ denotes the set of integers (positive, nonnegative integers), $\mathbb{R}\,(\mathbb{R}_{>0},\mathbb{R}_{\geq 0})$ denotes the set of real numbers (positive, nonnegative real numbers), $\mathbb{R}^n$ denotes the n-dimensional Euclidean space and $\mathbb{R}^{m\times n}$ the set of $m\times n$ real matrices. I denotes the identity matrices and, given $A\in\mathbb{R}^{n\times n}$, we use the compact notation $A\in\mathbb{R}^{n\times n}_{>0}(\mathbb{R}^{n\times n}_{<0})$ to represent a positive (negative) definite matrix. For a square matrix X, we denote $\mathrm{He}(X):=X+X^\top$. Given a sequence $x(t)$, $t\in\mathbb{Z}_{\geq 0}$, x^+ is a shorthand notation for $x(t+1)$. Function $\mathrm{sat}(\cdot)$ denotes the decentralized symmetric saturation function, *i.e.*, given $u\in\mathbb{R}^n$ and some bounds $\bar{u}_1,\dots,\bar{u}_n\in\mathbb{R}_{>0}$, $\mathrm{sat}(u):=(\max(\min(\bar{u}_1,u_1),-\bar{u}_1),\dots,\max((\bar{u}_n,u_n),-\bar{u}_n))$. Finally, $\overline{\mathrm{co}}\,\{v_r\in\mathbb{R}^n,\ r=1,\dots,n_v\}$ is the closed convex hull, *i.e.*, the smallest closed convex set that contains the points identified by the vectors v_r.

III. Preliminaries on anti-windup augmentation for discrete-time linear plants

In this section the general formulation of the direct linear anti-windup (DLAW) design for discrete-time plants is recalled, following the approach presented in [10].

Consider a plant (P) described by a linear discrete-time system in state-space form, *i.e.*,

$$(P)\quad \begin{cases} x_p^+ = A_p x_p + B_{p,u}u + B_{p,w}w \\ y = C_{p,y}x_p + D_{p,yu}u + D_{p,yw}w \\ z = C_{p,z}x_p + D_{p,zu}u + D_{p,zw}w, \end{cases} \tag{1}$$

where $x_p\in\mathbb{R}^{n_p}$ is the plant state, $u\in\mathbb{R}^{n_u}$ is the control input, $w\in\mathbb{R}^{n_w}$ is the exogenous input, $y\in\mathbb{R}^{n_y}$ is the measurable plant output and $z\in\mathbb{R}^{n_z}$ is the performance output. Assume that a controller (C) has been designed to achieve a desired level of performance in nominal conditions:

$$(C)\quad \begin{cases} x_c^+ = A_c x_c + B_{c,y}y + B_{c,w}w + v_1 \\ y_c = C_c x_c + D_{c,y}y + D_{c,w}w + v_2, \end{cases} \tag{2}$$

where $x_c\in\mathbb{R}^{n_c}$ is the controller state, $y_c\in\mathbb{R}^{n_u}$ is the controller output, $v_1\in\mathbb{R}^{n_c}$ and $v_2\in\mathbb{R}^{n_u}$ are additional inputs for AW augmentation. Clearly, when setting

$$u=y_c,\quad v_1=0,\quad v_2=0, \tag{3}$$

a basic requirement is that the *unconstrained* closed-loop system obtained by combining (1) and (2) is well defined and stable. Suppose now that the control input is subject to a saturation nonlinearity

$$u=\mathrm{sat}(y_c), \tag{4}$$

where $\mathrm{sat}(\cdot)$ is the saturation function defined in the notation section. The *constrained* closed-loop (*CCL*) system, obtained by combining (1), (2) and (4) with $v_1=0$ and $v_2=0$, is given by:

$$(CCL)\quad \begin{cases} x_{cl}^+ = A_{cl}x_{cl} + B_{cl,q}q + B_{cl,w}w \\ z = C_{cl,z}x_{cl} + D_{cl,zq}q + D_{cl,zw}w \\ y_c = C_{cl,u}x_{cl} + D_{cl,uq}q + D_{cl,uw}w, \end{cases} \tag{5}$$

$$q = dz(y_c), \tag{6}$$

where $dz(y_c):=y_c-\mathrm{sat}(y_c)$ is the deadzone nonlinearity, $x_{cl}=(x_p,x_c)\in\mathbb{R}^{n_p+n_c}$ and the corresponding matrices are reported in the appendix for completeness.

To handle the effect of saturation, the additional inputs v_1,v_2 are exploited by including an AW compensator, given by the following LTI system:

$$(AW)\quad \begin{cases} x_{aw}^+ = A_{aw}x_{aw} + B_{aw}(y_c-u) \\ \begin{bmatrix} v_1 \\ v_2 \end{bmatrix} = C_{aw}x_{aw} + D_{aw}(y_c-u), \end{cases} \tag{7}$$

where $x_{aw}\in\mathbb{R}^{n_{aw}}$ $(n_{aw}\geq 0)$, is the AW state and $(v_1,v_2)\in\mathbb{R}^{n_v}$ $(n_v=n_c+n_u)$. Matrices $A_{aw},B_{aw},C_{aw},D_{aw}$ determine the behavior of the AW compensator: as discussed in detail in the next section, the rationale behind their selection is to obtain a closed-loop system that delivers the performance of the unconstrained controller when operating in nominal conditions while guaranteeing a desirable relationship between the exogenous input w and the performance output z when saturation occurs.

The interconnection of (1), (2) and (7) through (4) can be expressed in compact form by combining (6) and the augmented closed-loop (*ACL*) system is given by

$$(ACL)\quad \begin{cases} x_a^+ = A_a x_a + B_{a,q}q + B_{a,w}w \\ z = C_{a,z}x_a + D_{a,zq}q + D_{a,zw}w \\ y_c = C_{a,u}x_a + D_{a,uq}q + D_{a,uw}w, \end{cases} \tag{8}$$

where $x_a:=(x_{cl},x_{aw})$ and the state space matrices are reported in the appendix.

IV. Performance oriented anti-windup synthesis for linear discrete-time systems

The majority of works in the framework of DLAW design [3] focus on the minimization of the ℓ_2 gain from w to z, by considering the class of ℓ_2 norm-bounded reference signals w (finite energy signals). As denoted in [5], such an approach to anti-windup design might not provide a satisfactory answer when addressing many practical control problems: indeed the ℓ_2 class is quite large and may not be well-suited to saturated systems whose performance level is expected to depend on the shape and the amplitude of the input signal. To overcome this intrinsic limitation, we propose a discrete-time version of the performance-oriented approach developed for continuous-time systems in [5].

A. Problem formulation

The main idea behind the AW performance-oriented strategy proposed in [5] is to exploit a reference model, which encodes the desired behavior of the closed-loop system, together with a suitable dynamic filter that allows generating or approximating reference signals of interest, according to the block diagram shown in Figure 1. First of all, a reference model (RM)

$$(RM) \quad \begin{cases} x_{rm}^+ = A_{rm}x_{rm} + B_{rm,w}w, \\ z_{rm} = C_{rm,z}x_{rm} + D_{rm,zw}w \end{cases} \tag{9}$$

is defined together with the performance output

$$z_e := z - z_{rm}, \tag{10}$$

which will be used to evaluate the mismatch between the reference and actual system responses. Specifically, we will assume in the following that the reference model coincides with the unconstrained closed-loop system, so that the purpose of the AW compensator will be to make the error z_e as small as possible when saturation occurs. Then, to achieve satisfactory time-domain performance to reference signals of interest which do not belong to the ℓ_2 norm-bounded class, an asymptotically stable LTI filter that approximates such signals is directly included in the augmented system. For instance, step references can be approximated by the output of the following LTI system:

$$(F) \quad w^+ = (1-\varepsilon)w, \quad w(0) = w_0, \quad \mathbb{R}_{>0} \ni \varepsilon \ll 1, \tag{11}$$

where w_0 denotes the initial condition of the filter and can be considered as the step amplitude. When combining equations (8)-(11), the following state space model is obtained:

$$\begin{cases} x^+ = Ax + B_q q \\ z_e = C_z x + D_{zq} q \\ y_c = C_y x + D_{yq} q \\ q = dz(y_c) \end{cases} \tag{12}$$

where $x := (x_a, x_{rm}, w) \in \mathbb{R}^{n_a+n_{cl}+n_w} =: \mathbb{R}^{n_x}$ and

$$A := \begin{bmatrix} A_a & 0 & B_{a,w} \\ 0 & A_{rm} & B_{rm,w} \\ 0 & 0 & (1-\varepsilon)I_{n_w} \end{bmatrix}, \quad B_q := \begin{bmatrix} B_{a,q} \\ 0 \\ 0 \end{bmatrix}, \tag{13}$$

$$C_z := \begin{bmatrix} C_{a,z} & -C_{rm,z} & D_{a,zw} - D_{rm,zw} \end{bmatrix}, \quad D_{zq} := D_{a,zq}, \tag{14}$$

$$C_y := \begin{bmatrix} C_{a,u} & 0 & D_{a,uw} \end{bmatrix}, \quad D_{yq} := D_{a,uq}. \tag{15}$$

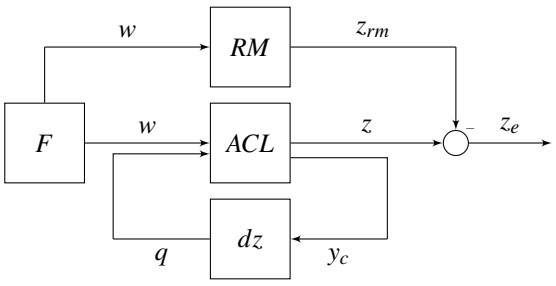

Figure 1. Block diagram for performance oriented synthesis.

Considering system (12), the design of the AW compensator can be associated with the solutions to the following problem.

Problem 1. *Find the smallest $\gamma \in \mathbb{R}_{>0}$ such that, given an initial state $x(0) = (0, 0, w_0)$, the following conditions are satisfied:*

- *$x(0)$ is inside the region of attraction of the origin of* (12)*;*
- *the following condition*

$$\sum_{t=0}^{\infty} z_e(t)^\top z_e(t) \le \gamma, \tag{16}$$

is satisfied for any $x(0)$ in the region of attraction of the origin of (12)*.*

B. Fixed-dynamics discrete-time anti-windup design

This section is devoted to presenting the main theoretical results of the paper. First of all, we state and prove the following theorem, which will be instrumental for the AW synthesis procedure to be provided next.

Theorem 1. *Consider the model reference AW system in* (12)*. If there exist matrices $Q = Q^\top \in \mathbb{R}_{>0}^{n_x \times n_x}$, $Y \in \mathbb{R}^{n_u \times n_x}$, $U \in \mathbb{R}_{>0}^{n_u \times n_u}$ (diagonal), and scalar $\gamma \in \mathbb{R}_{>0}$ such that the following conditions hold:*

$$\begin{bmatrix} -Q & -Y^\top + QC_y^\top & QC_z^\top & QA^\top \\ -Y + C_y Q & -2U + D_{yq}U + UD_{yq}^\top & UD_{zq}^\top & UB_q^\top \\ C_z Q & D_{zq}U & -\gamma I & 0 \\ AQ & B_q U & 0 & -Q \end{bmatrix} < 0, \tag{17}$$

$$\begin{bmatrix} \bar{u}_i^2 & Y_i \\ Y_i^\top & Q \end{bmatrix} \ge 0, \tag{18}$$

where $i = 1, \ldots, n_u$ and Y_i denotes the i-th row of Y, then the ellipsoid $\mathscr{E}(Q^{-1}) = \{x \in \mathbb{R}^{n_x} : x^\top Q^{-1} x \le 1\}$ is contained in the region of attraction of the origin of (12) *and the following bound holds:*

$$\sum_{t=0}^{\infty} z_e^\top z_e \le \gamma, \quad \forall x(0) \in \mathscr{E}(Q^{-1}). \tag{19}$$

Proof. The proof combines the steps used to derive the proof of the continuous-time version in [5] and some ideas borrowed from [10] to show that under the generalized sector condition used, *e.g.*, in [6], one can guarantee a decrease of a quadratic Lyapunov function along the dynamics of system (12). Before proceeding, note that the algebraic-loop is well-posed by virtue of the inequality $-2U + D_{yq}U + UD_{yq}^\top < 0$ (which is implied by (17)) and let us recall the following Lemma from [10], which will be exploited in the next steps.

Lemma 1. *For any diagonal matrix $M \in \mathbb{R}_{>0}^{n_u \times n_u}$ and $\forall y_c \in \mathbb{R}^{n_u}$, we have*

$$-2q^\top M(q - y_c + Hx) \ge 0, \quad \forall x \in \mathscr{L}(\bar{U}^{-1}H), \tag{20}$$

where $H \in \mathbb{R}^{n_u \times n_x}$, $\mathscr{L}(\bar{U}^{-1}H) := \{x \in \mathbb{R}^{n_x} : \|\bar{U}^{-1}Hx\|_\infty \le 1\}$ and $\bar{U} := diag(\bar{u}_1, \ldots, \bar{u}_{n_u})$.

Define now the matrices $P := Q^{-1}$, $M := U^{-1}$ and $H := YQ^{-1}$. Left- and right-multiplying LMI (17) by

$\mathrm{diag}(P,M,I_{n_z},I_{n_x})$ (congruence transformation) and then taking a Schur complement, one has:

$$\mathrm{He}\begin{bmatrix} \frac{A^\top PA-P}{2} & A^\top PB_q - H^\top M & 0 \\ MC_y & MD_{yq} + \frac{B_q^\top PB_q}{2} - M & 0 \\ C_z & D_{zq} & -\frac{\gamma}{2} I_{n_z} \end{bmatrix} < 0. \tag{21}$$

By applying again a Schur complement to the last column and row of (21), one also has

$$\mathrm{He}\begin{bmatrix} \frac{A^\top PA-P}{2} & A^\top PB_q - H^\top M \\ MC_y & MD_{yq} + \frac{B_q^\top PB_q}{2} - M \end{bmatrix} + \begin{bmatrix} C_z^\top \\ D_{zq}^\top \end{bmatrix} \frac{\begin{bmatrix} C_z & D_{zq} \end{bmatrix}}{\gamma} < 0. \tag{22}$$

By left- and right-multiplying (18) by $\mathrm{diag}(1,P)$, one obtains the equivalent set of LMIs

$$\begin{bmatrix} \bar{u}_i^2 & H_i \\ H_i^\top & P \end{bmatrix} \geq 0, \quad i = 1,...,n_u, \tag{23}$$

which imply that $\mathscr{E}(P) \subseteq \mathscr{L}(\bar{U}^{-1}H)$ (see, *e.g.*, [4]). At this point, consider a quadratic Lyapunov function $V(x) := x^\top Px$. Thanks to the implications of (23), by exploiting Lemma 1 we can write the following inequality $\forall x \in \mathscr{E}(P)$:

$$\Delta V + \frac{1}{\gamma} z_e^\top z_e \leq (x^+)^\top Px^+ - x^\top Px + \frac{1}{\gamma} z_e^\top z_e - 2q^\top M(q - y_c + Hx). \tag{24}$$

Substituting x^+ and z_e from equation (12) into the right hand side of (24) and using inequality (22), one verifies that

$$\Delta V + \frac{1}{\gamma} z_e^\top z_e < 0 \qquad \forall x \in \mathscr{E}(P) \setminus \{0\}, \tag{25}$$

from which it readily follows that

$$\Delta V < 0, \quad \forall x \in \mathscr{E}(P) \setminus \{0\}. \tag{26}$$

The above results implies that the set described by the ellipsoid $\mathscr{E}(P)$ is contained in the region of attraction of the equilibrium $x = 0$ and also that $\mathscr{E}(P)$ is contractively invariant [4]. Finally, noting from (25) that $\Delta V + \frac{1}{\gamma} z_e^\top z_e \leq 0 \forall x \in \mathscr{E}(P)$ and then summing this last inequality over t, one obtains:

$$\sum_{\tau=0}^{t} \Delta V(\tau) + \sum_{\tau=0}^{t} \frac{1}{\gamma} z_e(\tau)^\top z_e(\tau) = V(t) - V(0) + \sum_{\tau=0}^{t} \frac{1}{\gamma} z_e(\tau)^\top z_e(\tau). \tag{27}$$

Since $\mathscr{E}(P)$ is contractively invariant, $V(t) \leq 1 \ \forall t \geq 0$. When considering also that $V(t) \geq 0$ by definition, one obtains $V(t) - V(0) \leq 1 \ \forall t$ and therefore inequality (19) is easily derived from (27) and the proof is completed. □

Remark 1. *Theorem 1 provides useful tools for analysis purposes; on the other hand, for synthesis purposes, constraint* (17) *is bilinear in the decision variables U, Q and in the AW matrices, which are embedded in the definition of $A, B_q, C_z, D_{zq}, C_y, D_{yq}$. However, if the AW matrices A_{aw}, C_{aw} are known, equation* (17) *can be turned into a convex constraint using the same approach as [5]. To show this consider the bilinear terms $B_qU, D_{zq}U, D_{yq}U$. By expanding the products we get:*

$$B_qU = \begin{bmatrix} B_{cl,q}U + B_{cl,v}D_{aw}U \\ B_{aw}U \\ 0_{rm} \\ 0_{mw} \end{bmatrix}, \tag{28}$$

$$D_{zq}U = D_{cl,zq}U + D_{cl,zv}D_{aw}U, \tag{29}$$

$$D_{yq}U = D_{cl,uq}U + D_{cl,uv}D_{aw}U. \tag{30}$$

By using the following change of variables:

$$\hat{B}_{aw} := B_{aw}U, \quad \hat{D}_{aw} := D_{aw}U, \tag{31}$$

constraint (17) *is convex in the variables $U, Q, Y, \hat{B}_{aw}, \hat{D}_{aw}$ and the AW gains can be recovered as:*

$$B_{aw} = \hat{B}_{aw}U^{-1}, \quad D_{aw} = \hat{D}_{aw}U^{-1}. \tag{32}$$

Thanks to the considerations in Remark 1, one can exploit the results of Theorem 1 to guarantee desired properties to the augmented closed-loop system in which the AW matrices are computed according to the following algorithm.

Algorithm 1 (Performance-oriented AW synthesis)**.** *Find a fixed-dynamics anti-windup compensator following these steps:*

- *step 1: choose appropriate A_{aw} and C_{aw} (see Remark 3) and select a step input amplitude w_0 (in the multivariable case: $w_0 \in \mathbb{R}^{n_w}$);*
- *step 2: solve the following semidefinite program (SDP) in the variables Q, Y, U, γ, $\hat{B}_{aw}$, $\hat{D}_{aw}$:*

$$\textit{minimize} \quad \gamma, \tag{33}$$

$$\begin{bmatrix} -Q & -Y^\top + QC_y & QC_z^\top & QA^\top \\ -Y + C_yQ & L_{22} & L_{32}^\top & L_{42}^\top \\ C_zQ & L_{32} & -\gamma I & 0 \\ AQ & L_{42} & 0 & -Q \end{bmatrix} < 0, \tag{34}$$

$$\begin{bmatrix} \bar{u}_i^2 & Y_i \\ Y_i^\top & Q \end{bmatrix} \geq 0, \quad i = 1,...,n_u, \tag{35}$$

$$\begin{bmatrix} Q & \begin{bmatrix} 0 \\ \bar{w}_{0_i} \end{bmatrix} \\ \begin{bmatrix} 0 & \bar{w}_{0_i}^\top \end{bmatrix} & 1 \end{bmatrix} \geq 0, \quad i = 1,...,n_w, \tag{36}$$

where $\bar{w}_{0_i} = \begin{bmatrix} 0 & \cdots & w_{0_i} & \cdots & 0 \end{bmatrix}^\top \in \mathbb{R}^{n_w}$ (vector with the i-th *component of w_0 at the* i-th *index and zeros elsewhere) and the following definitions have been used:*

$$L_{22} := \mathrm{He}\left(-U + D_{cl,uq}U + D_{cl,uv}\hat{D}_{aw}\right), \tag{37}$$

$$L_{32} := D_{cl,zq}U + D_{cl,zv}\hat{D}_{aw}, \quad L_{42} := \begin{bmatrix} B_{clq}U + B_{cl,v}\hat{D}_{aw} \\ \hat{B}_{aw} \\ 0 \end{bmatrix}, \tag{38}$$

where matrix $0 \in \mathbb{R}^{(n_{rm}+n_w)\times n_u}$;

- *step 3: compute AW matrices as:*

$$B_{aw} = \hat{B}_{aw}U^{-1}, \qquad D_{aw} = \hat{D}_{aw}U^{-1}. \tag{39}$$

Remark 2. *The satisfaction of equation* (36) *guarantees that the initial condition* $x(0) = (0,0,w_0)$*, where* $w_0 \in W_0$ *with*

$$W_0 =: \overline{co}\left\{\chi_i \in \mathbb{R}^{n_w} : \chi_i^\top e_j = \begin{cases} w_{0_i} & \text{if } i = j \\ 0 & \text{if } i \neq j \end{cases}, i = 1,\dots,n_w\right\}, \tag{40}$$

is inside the region of attraction of the origin (12)*. In other words, the region of attraction contains a convex set whose vertices represent initial conditions corresponding to reference signals each made by a step of a given amplitude along one principal direction.*

Finally, the solution to Problem 1 is addressed by the following Theorem.

Theorem 2. *Given a set of* n_w *initial conditions* w_{0_i} *(step amplitudes), the closed-loop system* (12) *with an AW compensator constructed according to Algorithm 1 guarantees that:*

1) $\mathscr{E}(Q^{-1})$ *is a subset of the region of attraction of the origin;*
2) *the following inequality holds:*

$$\sum_{t=0}^{\infty} z_e^\top z_e \leq \gamma, \quad \forall x(0) \in \mathscr{E}(Q^{-1}), \tag{41}$$

where Q *and* γ *are the solutions of the SDP at step 2 of Algorithm 1;*

3) *the point* $x(0) = (0,0,w_0)$*, where* $w_0 \in W_0$*, is contained in the region of attraction;*

Proof. The proofs of items 1 and 2 follow immediately by applying Theorem 1 to the closed-loop system (12) with AW compensator computed according to Algorithm 1. The third item is a direct consequence of the conditions stemming from LMIs (36). □

Remark 3. *As noted in [5] for the continuous-time case, the main difficulty in Algorithm 1 is in the first step, namely, in appropriately selecting the AW matrices* A_{aw} *and* C_{aw}*. This choice may be carried out by considering the poles of the AW controller, which can be chosen,* e.g.*, by retaining a part of those obtained in a full order design case or by iterating from the static case until a satisfactory result is achieved (see, for additional details, [5, Algorithm 4.6]). An "almost" static approach, corresponding to a static compensator cascaded with a unit delay, is instead pursued in this work, as motivated and detailed in the next section.*

Remark 4. *The feasibility of the LMI conditions in Algorithm 1 is also strongly related to the size of the desired region of attraction* (40)*, which in turn depends on the amplitudes of the step signals along each axis (see Remark 2). In particular, the stabilization of the system will become more difficult as the required size of the region of attraction increases and at the same time a performance degradation (a larger mismatch* γ*) will be unavoidably observed (additional comments on this point can also be found in Section VI-C). Hence, a trade-off between stabilization for large references and closeness to the nominal reference model behavior must be accounted for during synthesis. As a preliminary step to Algorithm 1, one can try to find the largest region of attraction of the zero equilibrium for a given shape set of the initial condition without accounting for performance constraint (see,* e.g.*, [5, Remark 4.3] or [3, Algorithm 3]).*

V. Fixed-dynamics anti-windup design for algebraic loop avoidance

By inspecting equations (2), (4) and (7), one can observe that the AW signal v_2 is responsible for the presence of an algebraic loop in the controller dynamics, which must be avoided in real-time implementations [12]. Among the different approaches, delaying one sample as suggested in [7] is the simplest solution to handle such issue. For instance, when referring to a static AW compensator,

$$\begin{bmatrix} v_1 \\ v_2 \end{bmatrix} = \begin{bmatrix} D_{aw1} \\ D_{aw2} \end{bmatrix} q, \tag{42}$$

in which matrices D_{aw1}, D_{aw2} have been designed according to some criterion (see, *e.g.*, [10]), one would actually implement the AW dynamics as

$$\begin{cases} x_{aw}^+ = D_{aw2} q \\ v_1 = D_{aw1} q \\ v_2 = x_{aw}. \end{cases} \tag{43}$$

Not surprisingly, when passing from (42) to (43), performance and stability guarantees achieved by the synthesis process are lost. Hence, the approach proposed herein is to take into account the implemented structure of the AW compensator of equation (43) in the synthesis procedure. Such an approach would guarantee the designed performance and stability guarantees to the augmented closed-loop system at the expense of a small complexity increase with respect to purely static AW compensators. To this end, one can exploit the fixed-dynamics AW synthesis proposed in Section IV. Specifically, the structure of equation (43) corresponds to an AW compensator with

$$A_{aw} = 0, \quad B_{aw} = D_{aw2}, \quad C_{aw} = \begin{bmatrix} 0 \\ I_{n_u} \end{bmatrix}, \quad D_{aw} = \begin{bmatrix} D_{aw1} \\ 0 \end{bmatrix}. \tag{44}$$

It is worth noting that, in order to impose the compensator structure defined by (44), it is sufficient to define $\hat{D}_{aw} = \begin{bmatrix} \hat{D}_{aw1} \\ 0 \end{bmatrix}$, where $\hat{D}_{aw1} \in \mathbb{R}^{n_c \times n_u}$ becomes the new decision variable. In this case, D_{aw1} can be recovered as $D_{aw1} = \hat{D}_{aw1} U^{-1}$. Regarding the feasibility of this problem, note that A_{aw} in (44) is Schur stable and that the same considerations made in Remark 3 hold.

VI. Anti-windup augmentation for pitch-limited position control of multirotor UAVs

The experimental tests performed on a small quadrotor UAV are presented and discussed in this section. The tests are intended to show and compare the behavior of the control system with/without the AW augmentation in case saturation occurs. To this end, the experiment that we propose replicates operating conditions in which the quadrotor should not pitch too much with respect to the ground during maneuvering, *e.g.*, when high speeds should be avoided. Due to the specific underactuation mechanism in quadrotors, such vehicles have

to change their attitude in order to reach a desired position. In consolidated cascade-based control designs [13], the position controller acts as outer loop in charge of computing pitch and roll setpoints that should be tracked as fast as possible by the attitude controller, which plays the role of inner loop. Pitch limitations can therefore be obtained by saturating the output of the outer loop controller *i.e*, the pitch set-point: when such a controller includes an integral component, windup effects are likely to arise.

A. Quadrotor dynamics and baseline control

In this section we recall the dynamical model that is typically employed to control the position of multirotor UAVs. As we will enforce by design small angle set-points, the linearized dynamical model about hovering conditions can be considered to be sufficiently accurate for our purposes. In this case, the following model can be employed to describe the UAV longitudinal motion [1]:

$$\dot{x} = v_x, \qquad m\dot{v}_x = T_c\theta + d_x \tag{45}$$

$$\dot{\theta} = q, \qquad J\dot{q} = m_c + d_\theta \tag{46}$$

where $m, J \in \mathbb{R}_{>0}$ are the UAV mass and pitch inertia moment, respectively, $g = 9.81\text{m/s}^2$ is the gravity acceleration, $x, \theta \in \mathbb{R}$ are the position and the pitch angle, respectively, and $v_x, q \in \mathbb{R}$ are the corresponding translational and angular velocities. Finally, $m_c \in \mathbb{R}$ is the pitch control moment while $T_c \approx mg$ (hovering conditions) is the thrust magnitude and $d_x, d_\theta \in \mathbb{R}$ are unknown disturbances. As controlling the angular dynamics is of paramount importance to ensure closed-loop stability, it will be accurately characterized with a linear discrete-time black-box model identified from data collected in safe closed-loop experiments with the PBSID algorithm [14]. Hence, neglecting disturbances, the following discrete-time state space model will be used for control design purposes:

$$(Pos) \quad \begin{cases} x^+ &= x + T_s v_x \theta \\ v_x^+ &= v_x + gT_s \end{cases} \tag{47}$$

$$(Att) \quad \begin{cases} \theta^+ &= \theta + T_s q \\ x_a^+ &= A_q x_a + B_q m_c \\ q &= C_q x_a + D_q m_c \end{cases} \tag{48}$$

where $T_s \in \mathbb{R}_{>0}$ is the sampling time, A_q, B_q, C_q, D_q are matrices of appropriate dimension associated with the angular velocity dynamics state x_a.

As for the baseline control system, we make use of a cascade architecture employed by widely adopted multirotor autopilots [8] to control the translational motion (47). Such a strategy is motivated by observing that the translational dynamics can be indirectly controlled by changing the pitch angle, which enters the dynamics (47) through the term $gT_s\theta$. Specifically, θ is considered as a virtual input assigned by a saturated P-PID position controller, according to the control law

$$\theta_v(z) := PI_x(z)\left(k^o_{p,x}(x - x_d) - v_x\right) - D_x(z)v_x, \tag{49}$$

where $PI_x(z) := k^i_{p,x} + k^i_{i,x}T_s\frac{1}{z-1}$, $D_x(z) := k^i_{d,x}N^i_x\frac{z-1}{z-1+N^i_xT_s}$ are discrete transfer functions defining, respectively, a proportional-integral and (filtered) derivative action, and x_d is the desired position set-point. The pitch control moment m_c, which is the actual input of the system, is itself the output of a P-PID attitude controller, with the aim of tracking the virtual input θ_v assigned by the position loop. When plugging in (48) the inner loop controller, given, in state space form, by

$$\begin{cases} x^+_{c,a} &= A_{c,a}x_{c,a} + B_{c,aq}q + B_{c,a\theta}\theta + B_{c,av}\theta_v \\ m_c &= C_{c,a}x_{c,a} + D_{c,aq}q + D_{c,a\theta}\theta + D_{c,aq}\theta_v \end{cases} \tag{50}$$

one gets the following position-plus-attitude closed-loop model:

$$\begin{cases} x^+ &= x + T_s v_x \\ v_x^+ &= v_x + gT_s\theta \\ \theta^+ &= \theta + T_s q \\ x_a^+ &= A_q x_a + B_q(C_{c,a}x_{c,a} + D_{c,aq}q + D_{c,a\theta}\theta + D_{c,aq}\theta_v) \\ x^+_{c,a} &= A_{c,a}x_{c,a} + B_{c,aq}q + B_{c,a\theta}\theta + B_{c,av}\theta_v \end{cases} \tag{51}$$

where $q = C_q x_a + D_q(C_{c,a}x_{c,a} + D_{c,aq}q + D_{c,a\theta}\theta + D_{c,aq}\theta_v)$ and the role of θ_v as a virtual input is highlighted. Closing the loop with the outer controller (49), one gets the block diagram shown in Figure 2. Including a saturation at the output of the position controller, as shown in Figure 2, is equivalent to limiting the pitch angle set-point to the position-plus-attitude closed-loop system. Although placing a saturation on the set-point is not equivalent to imposing a hard constraint on the actual tilting of the platform, proper tuning of the attitude controller (50) guarantees that the UAV will hardly violate such a constraint.

B. Platform description

In this work, a lightweight custom quadrotor (take-off weight of about 230g) developed by the Aerospace Systems and Control Laboratory of Politecnico di Milano was employed for the experiments. The onboard autopilot, based on the open-source PX4 Pro firmware [8], features attitude and position controllers and estimators and has been customized using the ANT-X rapid prototyping system for multirotor control [15] to allow replacing the baseline attitude controller with user-defined controllers. The baseline control gains have been tuned using a structured H_∞ approach as detailed in [16] to achieve high performance in near hovering conditions.

To apply the AW techniques described in Section IV-B, both a baseline controller and a discrete-time state-space model of the attitude dynamics must be available. Following previous work on the same quadrotor [16], a second-order black-box model of the UAV pitch angular rate dynamics was identified with the PBSID subspace model identification algorithm using closed-loop experimental data [14].

C. Experimental results

In the experimental campaign, a maximum tilt angle of 10deg has been set to comply with possible limitations arising from the specific mission that the UAV has to perform,

[1]We just refer to the motion along the x direction as the same set of equations describes the motion along the y direction in the linearized case.

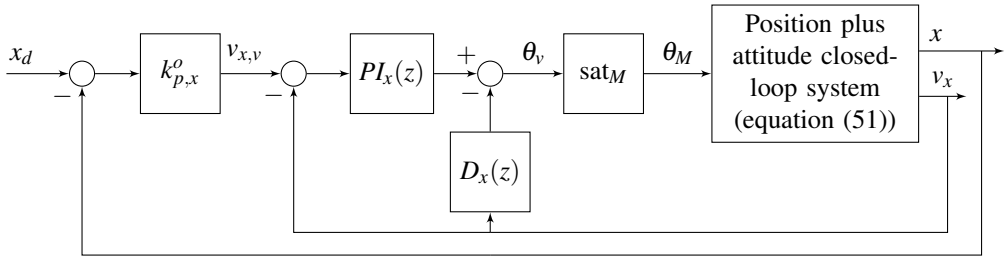

Figure 2. The longitudinal position controller with feed-forward and derivative action based on the plant measurements.

as mentioned at the beginning of this section. The AW compensator was tuned using Algorithm 1 in Section IV-B considering a step reference value (w_0) of 2m, which is a typical reference value for small quadrotors. The knowledge of all the matrices in equation (7) allows using Theorem 1 for the evaluation of the closed-loop properties in off-design conditions; in particular, for different step amplitudes w_0, the mimimum achievable γ (defined in equation (16)) with the obtained compensator can be computed. Figure 3 shows γ (scaled by T_s) as a function of the step reference w_0: the red line (dashed) is computed by using Theorem 1 while the blue line (solid) is obtained from time domain simulation data. As it clearly emerges, the result obtained using Theorem 1, which establishes stability and performance properties based on a quadratic function analysis, is too conservative [17] and it does not provide accurate results for large step references. Nevertheless, for medium amplitude signals (up to 3m) good results are predicted for the considered application. As can be noted, the intrinsic conservativity of the proposed method provides good robustness margins for off design operating conditions.

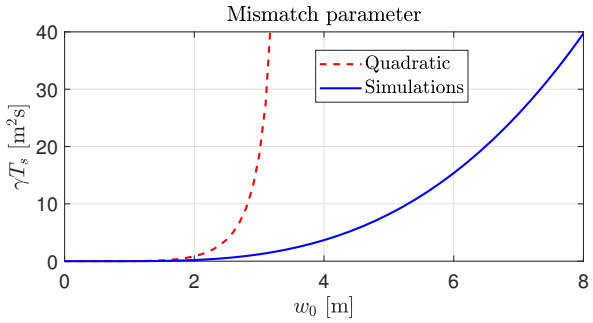

Figure 3. Scaled performance index as a function of the step amplitude.

The reference signal used to evaluate the effectiveness of the proposed augmentation in the experiments is a doublet with a period of 2.5s and amplitude $\pm$1m. Figure 4 compares the results, in terms of set-point tracking, obtained with the baseline and AW augumented controller. As can be observed, the compensator significantly reduces the overshoot in the response up to 20%, thereby improving the set-point tracking performance. It is also interesting to observe that the pitch angle limitation are respected in both cases (see Figure 5). Windup effects are clearly visible in Figure 5 in which it is shown that the baseline controller takes more time to change the UAV attitude when the final counter step is commanded. A video of the experiment is available at [18].

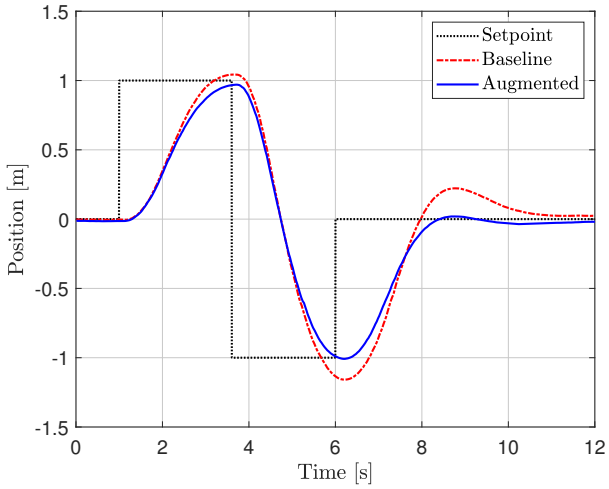

Figure 4. Position: baseline vs augmented controller (experiment).

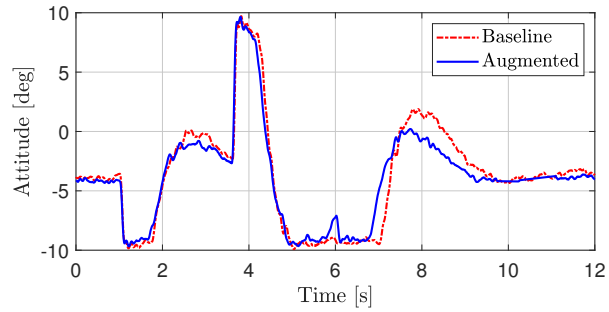

Figure 5. Pitch angle: baseline vs augmented controller (experiment).

Finally, we compare the experimental results with those of simulations, obtained using the model reported in equations (51) together with the identified pitch angle model. By inspecting Figure 6, one can appreciate the closeness between the predicted behavior and the one actually obtained in experiments, confirming the plausibility of the proposed modeling and control design. Of note, the non-null pitch angle observed at hovering (see Figure 5) is required to counteract an almost constant disturbance force d_x acting on the platform and induced by propellers misalignment. This issue magnifies windup effects (saturation is activated before what would happen in ideal conditions) and a disturbance force has been included in the simulation model to replicate such a condition. Finally, the mismatch between the amplitude of the overshoots

obtained in simulation and in experiments can be associated with the fact that no drag effects have been included in the simulation model.

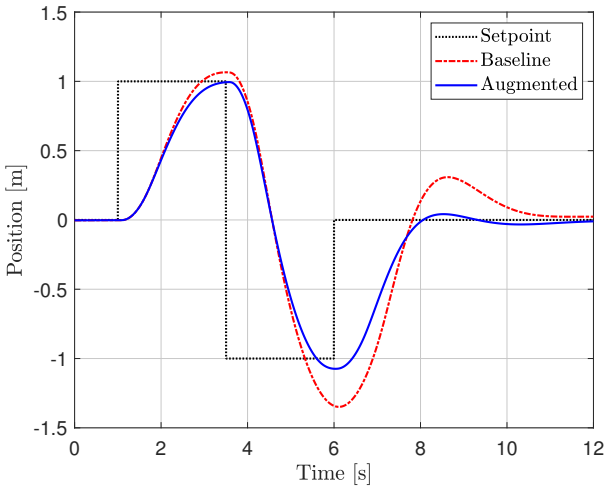

Figure 6. Position: baseline vs augmented controller (simulation).

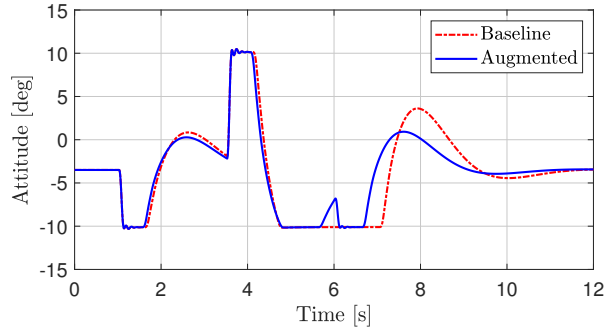

Figure 7. Pitch angle: baseline vs augmented controller (simulation).

VII. Conclusions

The problem of designing fixed-dynamics anti-windup compensators for saturated discrete-time linear systems has been addressed. With respect to the majority of modern AW methods, a performance-oriented approach has been considered by casting the AW design as a LMI-based optimization problem in which the performance index to be minimized represents the mismatch between the actual and the baseline closed-loop response, with the reference signal generated by a stable filter that approximates a signal of interest. The effectiveness of the proposed method has been proven in experiments to counteract windup effects in the position control of multirotor UAVs when saturation is included in the baseline controller design to limit the tilting of the UAV.

Appendix

Expressions of the matrices in system (5) **and** (8). For completeness we report the explicit expression of the matrices appearing in the constrained closed-loop system (5)

$$\left[\begin{array}{c|c} A_{cl} & \\ \hline C_{cl,z} & \\ \hline C_{cl,u} & \end{array}\right] := \left[\begin{array}{c|c} A_p + B_{p,u}\Delta_u D_{c,y} C_{p,y} & B_{p,u}\Delta_u C_c \\ \hline B_{c,y}\Delta_y C_{p,y} & A_c + B_{c,y}\Delta_y D_{p,yu} C_c \\ \hline D_{p,zu}\Delta_u D_{c,y} C_{p,y} + C_{p,z} & D_{p,zu}\Delta_u C_c \\ \hline \Delta_u D_{c,y} C_{p,y} & \Delta_u C_c \end{array}\right]. \tag{52}$$

$$\left[\begin{array}{c|c} B_{cl,q} & B_{cl,w} \\ \hline D_{cl,zq} & D_{cl,zw} \\ \hline D_{cl,uq} & D_{cl,uw} \end{array}\right] := \left[\begin{array}{c|c} -B_{p,u}\Delta_u & B_{p,w} + B_{p,u}\Delta_u \left(D_{c,y} D_{p,yw} + D_{c,w}\right) \\ \hline -B_{c,y}\Delta_y D_{p,yu} & B_{c,w} + B_{c,y} + \Delta_y \left(D_{p,yu} D_{c,w} + D_{p,yw}\right) \\ \hline -D_{p,zu}\Delta_u & D_{p,zw} + D_{p,zu}\Delta_u \left(D_{c,y} D_{p,yw} + D_{c,w}\right) \\ \hline I - \Delta_u & \Delta_u \left(D_{c,w} + D_{c,y} D_{p,yw}\right) \end{array}\right], \tag{53}$$

where $\Delta_u := (I - D_{c,y} D_{p,yu})^{-1}$, $\Delta_y := (I - D_{p,yu} D_{c,y})^{-1}$. The matrices in the augmented closed-loop system (8) are defined by

$$\left[\begin{array}{c|c|c} A_a & B_{a,q} & B_{a,w} \\ \hline C_{a,z} & D_{a,zq} & D_{a,zw} \\ \hline C_{a,u} & D_{a,uq} & D_{a,uw} \end{array}\right] := \left[\begin{array}{cc|c|c} A_{cl} & B_{cl,v} C_{aw} & B_{cl,q} + B_{cl,v} D_{aw} & B_{cl,w} \\ 0 & A_{aw} & B_{aw} & 0 \\ \hline C_{cl,z} & D_{cl,zv} C_{aw} & D_{cl,zq} + D_{cl,zv} D_{aw} & D_{cl,zw} \\ \hline C_{cl,u} & D_{cl,uv} C_{aw} & D_{cl,uq} + D_{cl,uv} D_{aw} & D_{cl,uw} \end{array}\right], \tag{54}$$

where

$$\left[\begin{array}{c|c} B_{cl,v} & \\ \hline D_{cl,uv} & \\ \hline D_{cl,zv} & \end{array}\right] := \left[\begin{array}{c|c} 0 & B_{p,u}\Delta_u \\ \hline I_{n_c} & B_{c,y}\Delta_y D_{p,yu} \\ \hline 0 & \Delta_u \\ \hline 0 & D_{p,zu}\Delta_u \end{array}\right]. \tag{55}$$

References

[1] A. Teel and N. Kapoor, "The $\mathscr{L}_2$ anti-windup problem: Its definition and solution," in *1997 European Control Conference (ECC)*, July 1997, pp. 1897–1902.

[2] G. Grimm, J. Hatfield, I. Postlethwaite, A. Teel, M. Turner, and L. Zaccarian, "Anti-windup for Stable Linear Systems With Input Saturation: An LMI-Based Synthesis," *IEEE Transactions on Automatic Control*, vol. 48, no. 9, pp. 1509 – 1525, 2003.

[3] S. Galeani, S. Tarbouriech, M. Turner, and L. Zaccarian, "A tutorial on modern anti-windup design," *European Journal of Control*, vol. 15, no. 3, pp. 418 – 440, 2009.

[4] Y. Li and Z. Lin, *Stability and Performance of Control Systems with Actuator Saturation*, 1st ed. Birkhäuser Basel, 2018.

[5] J.-M. Biannic and S. Tarbouriech, "Optimization and implementation of dynamic anti-windup compensators with multiple saturations in flight control systems," *Control Engineering Practice*, vol. 17, no. 6, pp. 703 – 713, 2009.

[6] J. G. da Silva Jr and S. Tarbouriech, "Anti-windup design with guaranteed regions of stability for discrete-time linear systems," *Systems and Control Letters*, vol. 55, no. 3, pp. 184 – 192, 2006.

[7] A. Syaichu-Rohman and R. Middleton, "Anti-windup schemes for discrete time systems: an LMI-based design," in *IEEE 5th Asian Control Conference*, vol. 1, July 2004, pp. 554 – 561.

[8] PX4-Community, "Documentation available at https://docs.px4.io/en/," Tech. Rep., 2018.

[9] M. Turner and I. Postlethwaite, "A new perspective on static and low order anti-windup synthesis," *International Journal of Control*, vol. 77, no. 1, pp. 27 – 44, 2004.

[10] M. Massimetti, L. Zaccarian, T. Hu, and A. Teel, "Linear discrete-time global and regional anti-windup: an LMI approach," *International Journal of Control*, vol. 82, no. 12, pp. 2179 – 2192, 2009.

[11] G. Grimm, A. R. Teel, and L. Zaccarian, "The l_2 anti-windup problem for discrete-time linear systems: Definition and solutions," *Systems & Control Letters*, vol. 57, no. 4, pp. 356 – 364, 2008.

[12] A. A. Adegbege and W. P. Heath, "A framework for multivariable algebraic loops in linear anti-windup implementations," *Automatica*, vol. 83, pp. 81 – 90, 2017.

[13] D. Invernizzi, M. Lovera, and L. Zaccarian, "Dynamic attitude planning for trajectory tracking in thrust-vectoring uavs," *IEEE Transactions on Automatic Control*, vol. 65, no. 1, pp. 453–460, 2020.

[14] G. van der Veen, J. van Wingerden, M. Bergamasco, M. Lovera, and M. Verhaegen, "Closed-loop subspace identification methods: an overview," *IET Control Theory Applications*, vol. 7, no. 10, pp. 1339–1358, Jul. 2013.

[15] ANT-X website, https://antx.it/.

[16] D. Invernizzi, S. Panza, and M. Lovera, "Robust Tuning of Geometric Attitude Controllers for Multirotor Unmanned Aerial Vehicles," *Journal of Guidance, Control and Dynamics*, vol. 43, pp. 1332–1343, 2020.

[17] T. Hu, A. Teel, and L. Zaccarian, "Stability and Performance for Saturated Systems via Quadratic and Nonquadratic Lyapunov Functions," *Automatica*, vol. 51, no. 11, pp. 1770 – 1786, 2006.

[18] P. Ghignoni, D. Invernizzi, and M. Lovera. Video of the experiments for "Fixed-dynamics anti-windup design: application to pitch-limited position control of multirotor Unmanned Aerial Vehicles". Youtube. [Online]. Available: https://youtu.be/RVBfSUirUv4